Time evolution of nonequilibrium photoexcited plasma in polar semiconductors

A. C. S. Algarte and R. Luzzi

Departamento de Física do Estado Sólido e Ciência de Materias, Instituto de Física, Universidade Estadual de Campinas,
13 100 Campinas, São Paulo, Brazil

The nonequilibrium thermodynamics and kinetics of evolution of relaxation processes in polar semiconductors under high levels of optical excitation is studied. This is done using a first-principles theory that allows for the determination of the nonlinear transport equations which describe the irreversible processes that develop in the media in typical pump-probe experiments. Numerical calculations are presented which permit a comprehensive discussion of measurements of ultrafast-time-resolved optical spectra of GaAs.

I. INTRODUCTION

A consequence of the technological development of laser and instrumentation has been a stepped-up effort devoted to the studies of the effects of high photoexcitation on semiconductor behavior. A considerable amount of information is available on the subject, and presently the growing interest in the development of quantum generators and other devices based on semiconductors at high density of excitations have made this topic one of the dominant fields in the area of semiconductor optics.[1] Studies of the optical properties of semiconductors under high-excitation conditions has shown novel and quite interesting features in optical spectroscopy.[2] The participation of nonequilibrium distribution of carriers and optical phonons is manifested in the behavior and shape of optical spectra. Work has been directed towards the aim of showing the possibility, in some cases, of describing the state of the photoexcited carriers solely by an effective temperature, a concept that has been applied rather more casually to the nonequilibrium distribution of LO phonons produced when hot electrons cascade down the band-energy states. This is a situation that can be accomplished in metals and doped semiconductors under steady constraints, e.g., constant fields, and the excitation are referred to as hot electrons; their state is characterized by an effective temperature, a concept originally due to Fröhlich.[3] However, the constraints imposed by excitation with a laser source are not of a steady-state nature, and, therefore, it is necessary to analyze the time evolution of the elementary excitations in the semiconductor plasma. This is the question we address here.

The highly excited plasma in semiconductors (HEPS) is a physical system with very many degrees of freedom in a far-from-equilibrium thermodynamic state. The statistical mechanics of irreversible processes, which deal with this kind of problem, has shown noticeable progress in recent years. A theory attempting to provide a unified description of nonequilibrium statistical mechanics is Jaynes's maximum-entropy formalism (MEF).[4] Methods based on this formalism were developed by Robertson[5] and Zubarev,[6] which allow for the derivation of nonlinear transport equations. Our analysis of the HEPS is built from the MEF using Zubarev's approach for the calculation of the transport equations. The time evolution of the macroscopic state of the HEPS is obtained for different typical experimental conditions. Theoretical results are compared with data obtained from time-resolved laser light spectroscopy.

These pump-probe experiments provide the optical response in situations when a mechanical perturbation is superimposed on the far-from-equilibrium HEPS. Hence irreversible processes develop in the system while it is probed, which are evidenced in the recorded spectra. The response function to be used in the analysis of the experiment should consequently be expressed in terms of the characteristics of the developing nonequilibrium state of the system. To this end, a method was devised within the framework of the MEF.[7] In order to apply this formalism, the nonequilibrium macroscopic state of the system needs to be described by a reduced set of thermodynamic variables. The equation for the response function is not closed in itself but coupled to proper transport equations for the nonequilibrium thermodynamic variables. These are the equations we are proposing and solving here for the HEPS.

In the next section we briefly describe the fundamentals of the method, in Sec. III we applied it to the study of polar semiconductors under strong laser light illumination, and Sec. IV is devoted to a discussion of the results and our conclusions.

II. THEORETICAL BACKGROUND

We briefly describe in this section the fundamentals of the MEF and related methods. The MEF permits one to deal with irreversible processes beginning from arbitrary nonequilibrium states, and incorporates from the onset nonlinear and nonlocal effects. For the cases of mechanical systems with very many degrees of freedom, the formalism can be looked upon as a generalization of Gibbs's ensemble algorithm. Let $\rho(t)$ be the nonequilibrium statistical operator (NSO) such that the nonequilibrium ensemble average of a dynamical quantity A is given by $\langle A \mid t \rangle = \mathrm{Tr}[A\rho(t)]$, a value to be placed in correspondence with the results of measurements performed on the actual physical system. The NSO is a functional of a basis set of dynamical quantities $\{P_1, P_2, \ldots, P_r\}$, in a contracted description of the system, whose nonequilibrium expectation values $\{Q_1(t), Q_2(t), \ldots, Q_r(t)\}$ (where $Q_j(t) = \mathrm{Tr}[P_j\rho(t)]$) correspond to the nonequilibrium thermodynamic variables that are observed and/or controlled in the experiment to be considered.

According to Bogoliubov,[8] a contracted description, when a reduced number of variables are enough to describe in a macroscopic way the state of the system is possible if there exists a relaxation time for microinformation, τ_μ, after which the system loses the memory of the initial distribution. The initial distribution, i.e., the one that should describe the system immediately after it is driven from equilibrium, depends on all the coordinates of the degrees of freedom, and its subsequent contraction is connected with the separation from the total Hamiltonian of strong interactions with certain symmetries.[9] These are symmetries related to the fast relaxing processes. Hence for not too short times, i.e., $t \gg \tau_\mu$, correlations with a lifetime smaller than τ_μ can be ignored, and the macroscopic state of the nonequilibrium system can be described by the reduced set of macrovariables $\{Q_j(t)\}$, $j = 1, 2, \ldots, r$. The choice of these macrovariables, or equivalently, that of the basis set of dynamical quantities $\{P_j\}$, is not universal but it depends on each concrete problem.[10] With increasing time scales, successive contractions of the basis set of dynamical quantities may be possible whenever there exists a hierarchy of relaxation times for subsets of macrovariables. These fundamental aspects of the theory become apparent, and are well illustrated, in the case of HEPS.

Once the basis set $\{P_j\}$ is chosen, the MEF requires access to information obtained at a given initial time, i.e., knowledge of the macrostate of the system. This information is built in the MEF statistical operator $\bar{\rho}$, defined as the one that satisfies the constraints

$$Q_j = \mathrm{Tr}(P_j\bar{\rho}) , \qquad (1)$$

and, subjected to these constraints and to normalization, makes maximum the MEF entropy

$$S = -\mathrm{Tr}(\bar{\rho}\ln\bar{\rho}) . \qquad (2)$$

The resulting statistical operator is

$$\bar{\rho} = \exp\left[-\phi - \sum_{j=1}^{r} F_j P_j \right] , \qquad (3)$$

where ϕ and $\{F_j\}$ are MEF Lagrange multipliers; the first ensures the normalization of $\bar{\rho}$ and the others are the intensive variables thermodynamically conjugated to the extensive macrovariable Q_j in the sense that

$$F_j = \frac{\partial S}{\partial Q_j} = F_j(Q_1, \ldots, Q_r), \quad j = 1, 2, \ldots, r . \qquad (4)$$

The thermodynamic parameters F's are a function of the expectation values Q's and Eqs. (4) can be considered as nonequilibrium equations of state. These relations can be inverted to obtain

$$Q_j = -\frac{\partial \phi}{\partial F_j} = Q_j(F_1, \ldots, F_r) , \qquad (5)$$

where

$$\phi(F_1, \ldots, F_r) = \ln\mathrm{Tr}\left[\exp\left[-\sum_{j=1}^{r} F_j P_j \right] \right] \qquad (6)$$

is the nonequilibrium Massieu-Planck functional or logarithm of the nonequilibrium partition function $\phi = \ln Z(F_1, \ldots, F_r)$. The MEF fully extends the entire equilibrium thermodynamic formalism for use on nonequilibrium systems, no matter how far from equilibrium, and it is completely compatible with nonlinear nonequilibrium thermodynamics.[11]

The equations of evolution for the macrovariables $Q_j(t)$ or generalized transport equations (GTE) are

$$\frac{dQ_j(t)}{dt} = \frac{d}{dt}\langle P_j \mid t \rangle = \mathrm{Tr}\{(i\hbar)^{-1}[P_j, H]\rho(t)\} , \qquad (7)$$

and to close the formalism an expression for the NSO $\rho(t)$ needs to be obtained. The NSO should satisfy the Liouville equation, for isolated systems, and is a functional of $\bar{\rho}$, which fixes the initial conditions. There are several methods to obtain $\rho(t)$ in terms of the MEF distribution $\bar{\rho}$,[5,6,9] associated with different forms of projection operators P, which separate the NSO at all moments of time

$$\rho = P\rho + (1-P)\rho = \bar{\rho} + (\rho - \bar{\rho})$$

into a secular nondissipative term $\bar{\rho}$, and another

that carries on irreversible behavior. In Zubarev's approach the NSO, corresponding to the initial value problem, with initial condition $\bar{\rho}$, is defined by

$$\rho_\epsilon(t) = \exp\left[\epsilon \int_{-\infty}^{t} dt' \, e^{\epsilon(t'-t)} \ln\bar{\rho}(t', t'-t)\right] ,$$

(8)

with $\epsilon \rightarrow 0+$ after the trace operation in the calculation of averages has been performed. In this equation the first term in the argument of $\bar{\rho}$ stands for the time dependence on the parameters $F(t)$, whereas the second denotes the dependence on time of operators P in the Heisenberg picture.

NSO (8) satisfies the equation

$$\frac{\partial}{\partial t} \ln\rho_\epsilon + i\mathcal{L} \ln\rho_\epsilon = -\epsilon(\ln\rho_\epsilon - \ln\bar{\rho}) ,$$

(9)

which is a Liouville equation with infinitesimal sources, and $\mathcal{L}$ is the Liouville operator of the system, i.e., $\hbar^{-1}$ times the commutator with H. The source in Eq. (9) selects the retarded solutions of the Liouville equation corresponding to the condition given at the initial time by $\bar{\rho}$, i.e., the constraints imposed by the given experimental situation. Hence Zubarev's method introduces from the onset irreversible macroscopic evolution of the system through a breaking of the time-reversal symmetry of the Liouville equation.[12] The choice in Eq. (8) of the initial reference time in the remote past and the use of the convergence factor $\exp(\epsilon t)$ eliminates undesirable transients; this satisfies the requirement that the treatment is valid for times $t \gg \tau_\mu$.[13]

NSO (8) can be separated in the form $\rho_\epsilon = \bar{\rho} + (\rho_\epsilon - \bar{\rho})$, composed of a nondissipative term and another describing irreversible producing processes, where

$$\bar{\rho}(t) = \exp\left[-\phi(t) - \sum_{j=1}^{r} F_j(t) P_j\right] ,$$

(10a)

$$\rho_\epsilon - \bar{\rho} = \int_0^1 du \, Y(\zeta \mid u)(\bar{\rho})^{-u} \zeta (\bar{\rho})^{u+1} ,$$

(10b)

$$Y(\zeta \mid x) = 1 + \int_0^x du \, Y(\zeta \mid u)(\bar{\rho})^{-u} \zeta (\bar{\rho})^u ,$$

(10c)

$$\zeta(t) = -\int_{-\infty}^{0} dt' \, e^{\epsilon t'} \frac{d}{dt'} \ln\bar{\rho}(t+t', t') .$$

(10d)

With these results the GTE's (7) are

$$\frac{dQ_j(t)}{dt} = \langle \dot{P}_j \mid t \rangle_0 + \sum_{k=1}^{r} \int_{-\infty}^{0} dt' \, e^{\epsilon t'} \{[\dot{P}_j; \dot{P}_k \mid t] F_k(t+t') + [\dot{P}_j; P_k \mid t] \dot{F}_k(t+t')\} ,$$

(11)

where

$$[A;B \mid t] = \int_0^1 du \, \langle A Y(\zeta \mid u)(\bar{\rho})^{-u} \Delta B(\bar{\rho})^u \mid t \rangle_0$$

(12)

is a generalized correlation function of quantities A and B, $\Delta B = B - \langle B \mid t \rangle_0$, and $\langle f \mid t \rangle_0 = \text{Tr}[f\bar{\rho}(t)]$.

Let us observe that the right-hand side of Eq. (11) depends explicitly on the thermodynamic parameters $F(t)$ and implicitly on the macrovariables $Q(t)$ via the state equations (4) or (5), and therefore it is convenient to go over a set of equations for them. Using Eqs. (7) and (5) we write

$$\frac{dQ_j}{dt} = -\sum_k \frac{\partial^2 \phi}{\partial F_j \partial F_k} \frac{dF_k}{dt} = -\sum_k (P_j; P_k \mid t) \dot{F}_k ,$$

(13)

and inversion of this system of equations provides the alternative set of GTE's:

$$\frac{dF_j}{dt} = -\sum_k C_{jk}^{-1}(t) \langle (i\hbar)^{-1} [P_k, H] \mid t \rangle ,$$

(14)

where C^{-1} is the inverse of the correlation matrix

$$C_{jk}(t) = (P_j; P_k \mid t)$$

$$= \int_0^1 du \, \langle P_j(\bar{\rho})^{-u} \Delta P_k(\bar{\rho})^u \mid t \rangle_0 .$$

(15)

GTE's (11) or (12) are highly nonlinear integrodifferential equations whose solutions, for given initial conditions, determine the irreversible evolution of the macroscopic state of the system. The method is closed at this point, and in conclusion we may say that, for systems governed by Hamiltonian dynamics, methods based on the MEF provide a way to describe the thermodynamic evolution and behavior of far-from-equilibrium systems for a large class of experimental situations. We proceed next to apply the method to the study of optically excited nonequilibrium plasma in semiconductors.

III. TIME EVOLUTION OF HOT PHOTOEXCITED PLASMA IN SEMICONDUCTORS

Studies of optical properties of semiconductors under high-excitation densities provide measurements of the effective temperature of hot carriers[2,14,15] and determination of the distribution functions of hot phonons generated by the photoexcited carriers cascading down the band-energy

states.[2,16,17] Based on the method described in Sec. II, we present here a study of the evolution of the nonequilibrium thermodynamic state of the HEPS under different experimental conditions. In this study a direct-band-gap polar semiconductor is illuminated by intense laser radiation, and a concentration of electron-hole pairs is being created in single or double photon absorption processes. Optical spectra (time resolved or time integrated) are recorded while the HEPS is relaxing its energy excess through different channels. The system Hamiltonian is composed of the electron energy operator; i.e., Bloch-bands Hamiltonian and Coulomb interaction energy, the Hamiltonians of the phonon and photon fields, the interaction energies of electrons with lattice vibrations (deformation potentials and Frölich interactions), and radiation, using the dipole approximation for the latter, and anharmonic interactions between lattice modes. They are well known, and therefore we omit listing them here. For the Bloch Hamiltonian we consider only two inverted bands, and the effective-mass approximation for describing the dynamics of electrons in conduction and valence bands is used. Further, we resort to the electron-hole representation.

Next, according to the MEF, to describe the non-equilibrium macroscopic state of the system it is necessary to choose a basis set of dynamical quantities $\{P_j\}$. This requires an analysis of the hierarchy of relaxation times referred to in Sec. II. First, we assume that local lattice heating on the focal zone of the laser beam can be neglected, i.e., experimental conditions are supposed to be such as to keep acoustical phonons in fairly constant equilibrium, throughout the sample, with a heat reservoir at temperature T_0. Second, we neglect stimulated recombination and self-absorption, which give no relevant contribution except near equilibrium conditions that are exempted from our discussion. The radiation field associated with spontaneous recombination is incorporated in the carrier Hamiltonian, and the laser field is characterized by its photon energy and power. Thus variables for the photon and acoustical phonon subsystems need not be included into the basis set of macrovariables. The NSO can be factorized into the direct product of the distribution function of the external subsystems of laser and A phonons, and the relevant one corresponding to the open system of carriers and LO phonons. We derive GTE's for a proper set of variables of the open system under the constraints imposed by contact with a thermal reservoir and laser illumination.[18]

The photoinjected carriers attain a very rapid internal thermalization due to the strong Coulomb interaction; this occurs in the subpicosecond time scale for the levels of excitation we are going to con-

sider here. Hence, for times larger than a tenth of a picosecond, the contracted description of the carrier subsystems can be done in terms of the carrier Hamiltonian $P_1 = H_c$, and the number operators for electrons and holes $P_2 = N_e$ and $P_3 = N_h$, since electron-hole pairs are created in laser light absorption and annihilated in recombination processes. The thermodynamically conjugated parameters will be written

$$F_1(t) = \beta(t) = [k_B T(t)]^{-1},$$

$$F_2(t) = -\beta(t)\mu_e(t),$$

and

$$F_3(t) = -\beta(t)\mu_h(t),$$

where $T(t)$ is to be interpreted as the quasitemperature of carriers and μ_e and μ_h as the quasichemical potentials, respectively, of electrons and holes having effective masses m_e and m_h.

The LO phonons are produced by relaxation of the hot carriers at large rates in the early stages following the initial departure from equilibrium. This rate of production is larger when the phonon wave number is smaller.[16] As a consequence, differently to the case of the carrier system, a contracted description of the LO-phonon subsystem in terms of solely its energy—and the associated quasi-temperature—should not be an appropriate one for very short times after initial excitation. Experimental and theoretical evidence[16,17,19] show that internal thermalization of LO-phonon modes occurs with the different modes coming successively in equilibrium with the carrier system. Next the composed system relaxes towards final equilibrium with the lattice with a long delay time, unless the number of LO phonons in excess of equilibrium is not large, as we will see later on. Therefore, for the initial stage, following the beginning of photoexcitation and the period of microrandomization, a suitable description of the macroscopic state of LO phonons would be in terms of the set of occupation numbers $\nu_{\vec{q}} = b_{\vec{q}}^{\dagger} b_{\vec{q}}$, with $\vec{q}$ running over the entire Brillouin zone. The associated nonequilibrium MEF thermodynamic parameters can be taken as $F_{\vec{q}}(t) = \hbar\omega_{\vec{q}}/k_B T_{\vec{q}}(t)$, defining a quasitemperature for each mode.[16] A second stage sets in at the time of the near thermalization of LO-phonon modes and carriers, and then a contracted description of the LO-phonon system can be performed with its Hamiltonian $P_4 = H_{LO}$ as the relevant dynamical quantity and the inverse quasi-temperature

$$F_4(t) = \beta_{LO}(t) = [k_B T_{LO}(t)]^{-1}$$

as the conjugated thermodynamic parameter. Typi-

cal times for the realization of this second kinetic stage are of the order of a few to tens of picoseconds depending on experimental conditions.[19]

The contracted description based on $\{H_c, N_e, N_h, H_{LO}\}$ can also be used to study the first kinetic stage, but then it needs to be complemented with the calculation of the correlation functions that give the distribution functions $v_{\vec{q}}(t) = \langle v_q | t \rangle$, for example, using the method of Ref. (7).[19] This complementarity between GTE and equations for correlation functions, in order to obtain a complete description of the state of the system in the different kinetic stages, has been discussed by Kalashnikov.[10]

We carry on the study of the nonequilibrium thermodynamics of the HEPS using the basis set $\{H_c, N_e, N_h, H_{LO}\}$ and its conjugated variables

$$\{\beta(t), -\beta(t)\mu(t), -\beta(t)\mu_h(t), \beta_{LO}(t)\} ,$$

therefore given the description of the second kinetic stage. However, we use the same basis for the first

kinetic stage also, and then it must be kept in mind that the results thus obtained are a low-order approximation, whose merits will be discussed in each case to be considered.

With the use of the aforementioned basis set of dynamical quantities, the auxiliary MEF statistical operator is

$$\bar{\rho} = \exp[-\phi - \beta(H_c - \mu_e N_e - \mu_h N_h) - \beta_{LO} H_{LO}] ,$$

(16)

and we write, for GTE's

$$\sum_{k=1}^{4} (P_j; P_k \,|\, t) \dot{F}_k(t) = -\langle (i\hbar)^{-1}[P_j, H] \,|\, t \rangle$$

$$= \sum_{l=0}^{\infty} J_j^{(l)}(t) ,$$

(17)

with $j = 1-4$, and the last term is an expansion in terms of collision operators,[20] where

$$J_j^{(0)} = (i\hbar)^{-1} \langle [H_0, P_j] \,|\, t \rangle_0 ,$$

(18a)

$$J_j^{(1)} = (i\hbar)^{-1} \langle [H', P_j] \,|\, t \rangle_0 ,$$

(18b)

$$J_j^{(2)} = (i\hbar)^{-2} \int_{-\infty}^{0} dt' e^{\epsilon t'} \left\langle \left[H'(t'), [H', P_j] + i\hbar P_k \frac{\partial J_j^{(1)}}{\partial Q_k} \right] \, \middle| \, t \right\rangle_0 .$$

(18c)

Here H_0 is the Hamiltonian of the free systems, and H' is the interaction energy operator of carriers with the phonon and radiation fields when P_j is H_c, N_e, and N_h, and interaction energy of LO phonons with carriers and anharmonic interaction when P_j is H_{LO}. Scattering operators $J_j^{(0)}$ and $J_j^{(1)}$ are null, and we truncate the expansion in second order, i.e., we retain only the contribution $l = 2$. This is the so-called quasilinear approximation in the relaxation processes: It is equivalent to take $Y = 1$ in Eq. (10b) keeping interactions up to second order in the coupling strengths.

The scattering operator $J_1^{(2)}$ contains contributions due to scattering by acoustic and LO phonons and interaction with the radiation fields; the cross terms are null. These partial scattering operators are

$$J_{1n}^{(2)}(t) = \frac{2\pi}{\hbar} \sum_{\alpha} \sum_{\vec{k}, \vec{q}} |U_\alpha^n(\vec{k}, \vec{q})|^2 (\epsilon_{\vec{k}+\vec{q}}^\alpha - \epsilon_{\vec{k}}^\alpha) \{ (v_{\vec{q}}^n + 1) f_{\vec{k}+\vec{q}}^\alpha(t)[1 - f_{\vec{k}}^\alpha(t)]$$

$$- v_q^n f_k^\alpha(t)[1 - f_{k+1}^\alpha(t)] \} \delta(\epsilon_{k+q}^\alpha - \epsilon_k^\alpha - \hbar\omega_q^n) ,$$

(19)

where $n = A$ or LO, and α is e or h. In these equations v^n are the phonon distribution functions

$$v_{\vec{q}}^A = [\exp(\beta_0 \hbar\omega_q^A) - 1]^{-1} ,$$

(20a)

$$v_{\vec{q}}^{LO} = v_{LO}(t) = \{\exp[\beta_{LO}(t)\hbar\omega_0] - 1\}^{-1} ,$$

(20b)

where we use a dispersionless frequency for LO phonons, and $\omega_q^A = sq$, with s the sound velocity,

$$f_k^\alpha(t) = (\exp\{\beta(t)[\epsilon_k^\alpha - \mu_\alpha(t)]\} + 1)^{-1}$$

(20c)

are Fermi-Dirac functions, and $\epsilon_{\vec{k}}^e = E_G + \hbar^2 k^2 / 2m_e$ and $\epsilon_{\vec{k}}^h = \hbar^2 k^2 / 2m_h$. The interaction matrix elements are

$$|U_\alpha^{LO}(\vec{k}, \vec{q})|^2 = \frac{2\pi e^2 \hbar\omega_0}{V}(\epsilon_\infty^{-1} - \epsilon_0^{-1}) q^{-2} \epsilon^{-2}(\vec{q}; t) ,$$

(21a)

$$|U_\alpha^A(\vec{k}, \vec{q})|^2 = \frac{E_\alpha^2 \hbar q}{2\rho V s} ,$$

(21b)

where V is the active sample volume, ϵ_0 and ϵ_∞ are the static and high-frequency dielectric constants, E_α is the deformation potential interaction couplings, ω_0 is the dispersionless LO-phonon frequency, ρ is the material density, and $\epsilon(\vec{q}; t)$ is the q-wave-number static dielectric constant. The latter accounts for the screening of the bare Frölich in-

teraction, and we use for it the random-phase approximation result

$$\epsilon(\vec{q};t)\simeq 1+\frac{q_0(t)}{q^2}$$

with

$$q_0^2(t)=\frac{4\pi e^2}{V}\sum_{\vec{k},\alpha}\left|\frac{\partial f_k^{\alpha}(t)}{\partial\epsilon_k^{\alpha}}\right| . \tag{22}$$

Note that q_0 is dependent on the thermodynamic

parameters $\beta(t)$ and $\mu(t)$ and, therefore, needs to be determined self-consistently. In the numerical applications presented in the next section, this is automatically incorporated in the computer program; an explicit analysis of the effects of screening due to polarization of the photogenerated carrier gas on the rate of energy relaxation is underway and will be reported elsewhere.

The partial scattering operators involving the interaction with luminescence and laser radiation are, respectively,

$$J_{1R}^{(2)}(t)=\frac{2\pi}{\hbar}\sum_{\vec{k},\vec{q}}|U^R(\vec{k},\vec{q})|^2(\epsilon_{\vec{k}}^e+\epsilon_{\vec{k}}^h)f_{\vec{k}}^e(t)f_{\vec{k}}^h(t)\delta(\epsilon_{\vec{k}}^e+\epsilon_{\vec{k}}^h-c\epsilon_{\infty}^{-1/2}q) \tag{23}$$

and

$$J_{1L}^{(2)}(t)=\frac{2\pi}{\hbar}\sum_{\vec{k}}|U^L(\vec{k},\vec{q})|^2(\epsilon_{\vec{k}}^e+\epsilon_{\vec{k}}^h)[1-f_k^e(t)-f_k^h(t)]\delta(\hbar\Omega_L-\epsilon_k^e-\epsilon_k^h) . \tag{24}$$

The interaction matrix elements are

$$|U^R(\vec{k},\vec{q})|^2=\frac{e^2\hbar E_G}{2\epsilon_{\infty}Vm_xcq} , \tag{25a}$$

and Eq. (24) is rewritten as

$$J_{1L}^{(2)}(t)=V[1-f_L^e(t)-f_L^h(t)]\hbar\Omega_L\times\begin{cases}\alpha_1^0 I_L(t)/\hbar\omega_L & \tag{25b}\\ \alpha_2^0 I_L^2(t)/\hbar\omega_L, & \tag{25c}\end{cases}$$

where E_G is the energy gap, I_L is the flux of laser power,

$$f_L^e(t)=\left\{\exp\left[\beta(t)\left[\frac{m_x}{m_e}(\hbar\Omega_L-E_G)+E_G-\mu_e(t)\right]\right]+1\right\}^{-1} ,$$

$$f_L^h(t)=\left\{\exp\left[\beta(t)\left[\frac{m_x}{m_h}(\hbar\Omega_L-E_G)-\mu_h(t)\right]\right]+1\right\}^{-1} ,$$

and α_1^0 and α_2^0 are the one-photon and two-photon absorption coefficients, whose experimental values are used when numerial applications are done. Ω_L is once or twice the laser frequency ω_L in one- or two-photon absorption processes, respectively.

Furthermore,

$$J_2^{(2)}(t)=J_3^{(2)}=\frac{2\pi}{\hbar}\sum_{\vec{k},\vec{q}}|U^R(\vec{k},\vec{q})|^2 f_{\vec{k}}^e(t)f_{\vec{k}}^h(t)\delta(c\epsilon_{\infty}^{-1/2}q-\epsilon_{\vec{k}}^e-\epsilon_{\vec{k}}^h)+(\hbar\Omega_L)^{-1}J_{1L}^{(2)}(t) , \tag{26}$$

$$J_4^{(2)}(t)=-J_{1LO}^{(2)}(t)+J_{4AN}^{(2)}(t) , \tag{27}$$

where the first term on the right-hand side is minus the contribution to the partial scattering operator for variation of carrier energy due to collisions with LO phonons, and

$$H_{4AN}^{(2)}(t)=N\tau^{-1}\hbar\omega_0[\nu_{LO}(t)-\nu_{LO}^0] \tag{28}$$

is the contribution due to anharmonic effects in lowest order, with ν_{LO}^0 being the equilibrium distribution function N is the number of unit cells (V/V_{cell}), and

$$\tau^{-1}=\frac{2\pi}{\hbar^2 N}\sum_{\vec{q},\vec{q}',\vec{q}'}|\phi|^2(1+\nu_{\vec{q}'}^A+\nu_{\vec{q}''}^A)$$

$$\times\delta(\omega_0-\omega_{\vec{q}'}^A-\omega_{\vec{q}''}^A)\delta_{\vec{q},\vec{q}'+\vec{q}''} . \tag{29}$$

Here ϕ are the matrix elements for anharmonic processes involving three phonons (one LO decaying into two A phonons). Relaxation time τ is the only

free parameter in the theory.

The different elements of the correlation matrix that appear on the left-hand side of Eq. (17) are

$$(H_c; H_c \mid t) = \sum_{\vec{k}, \alpha} (\epsilon_{\vec{k}}^{\alpha})^2 f_{\vec{k}}^{\alpha}(t) [1 - f_{\vec{k}}^{\alpha}(t)] , \qquad (30a)$$

$$(H_c; N_\alpha \mid t) = \sum_{\vec{k}} \epsilon_{\vec{k}}^{\alpha} f_{\vec{k}}^{\alpha}(t) [1 - f_{\vec{k}}^{\alpha}(t)] = (N_\alpha; H_c \mid t) , \qquad (30b)$$

$$(N_\alpha; N_\alpha \mid t) = \sum_{\vec{k}} f_{\vec{k}}^{\alpha}(t) [1 - f_{\vec{k}}^{\alpha}(t)] , \qquad (30c)$$

$$(H_{LO}; H_{LO} \mid t) = N(\hbar\omega_0)^2 \nu_{LO}(t) [1 + \nu_{LO}(t)] . \qquad (30d)$$

We note however, that the GTE involve the quasi-chemical potentials $\mu_{e,h}(t)$, but a more accessible experimental data is the carrier concentration $n(t)$. The quasichemical potentials are related to it and quasitemperature $T(t)$ by the known relations

$$n(t) = n_e^0(t) F_{1/2}(\beta(t)[\mu_e(t) - E_G])$$
$$= n_h^0(t) F_{1/2}(\beta(t)\mu_h(t)) , \qquad (31)$$

where $n_\alpha^0(t) = 2(2\pi m_\alpha / \beta \hbar^2)^{3/2}$ and F is the Fermi function of index $\frac{1}{2}$.

The coupled system of nonlinear integrodifferential GTE's (17) can now be solved for each given experiment using correlation functions (30) and scattering operators (23) to (28), and considering Eq. (31). A unique solution of the GTE's follows once the initial conditions are given, in the present case the values of T, T_{LO}, and n at the time when randomization of microprocesses has occurred, and the method can be applied, as discussed in Sec. II. From then on the GTE's describe the irreversible evolution of the nonequilibrium HEPS, and comparison of theoretical and experimental results should provide the physical picture of the kinetics of relaxation processes in the system. In the next section we applied the results thus obtained to the study of several experimental situations, namely optical measurements in photoexcited GaAs samples.

IV. NONEQUILIBRIUM THERMODYNAMICS OF GaAs

Let us consider a GaAs sample under intense laser illumination with photoinjected carriers being produced in one- or two-photon absorption processes. This applies to the situations when $\hbar\omega_L > E_G$ and $\hbar\omega_L < E_G$, but $2\hbar\omega_L > E_G$, respectively; two-photon absorption allows for excitation in the bulk of the sample and it shows to be an efficient excitation process.[21] In Table I we present the values of different

TABLE I. Characteristic parameters of GaAs used in the numerical calculations.

$\hbar\omega_0 = 37$ meV[a]	$\alpha_2^0 = 0.02$ cm/MW[d]
$\epsilon_0 = 12$[a]	$E_e = 7.0$ eV[e]
$\epsilon_\infty = 11$[a]	$E_h = 3.5$ eV[e]
$m_e = 0.068 m_0$[b]	$V_{cell} = 1.8 \times 10^{-22}$ cm[3b]
$m_h = 0.5 m_0$[b]	$\rho = 5.31$ g/cm[3f]
$E_g(0) = 1.52$ eV[c,b]	$s = 5.22 \times 10^5$ cm/s[f]

[a]J. D. Dow and D. Redfield, Phys. Rev. B **2**, 594 (1972).
[b]S. M. Sze, *Physics of Semiconductor Devices* (Wiley-Interscience, New York, 1969).
[c]Dependence of gap on temperature $E_G(T) = E_G(0) - 5.8 \times 10^{-4} T^2 (T + 300 \text{ K})^{-1}$.
[d]J. M. Ralston and R. K. Chang, Appl. Phys. Lett. **15**, 164 (1969).
[e]C. Jacoboni and L. Reggiani, Adv. Phys. **28**, 493 (1979).
[f]B. R. Nag, *Theory of Electrical Transport in Semiconductors* (Pergamon, New York, 1972).

characteristic parameters of GaAs which are used in the numerical calculations. We consider in all cases a rectangular pumping laser pulse of very short duration (in the picosecond scale) with a single pulse isolated from the train of pulses, and we follow the evolution of the HEPS during pulse action and after pulse relaxation to equilibrium.

We consider the system in the conditions of the experiments of Refs. 22–24, where fast-time-resolved spectroscopy measurements are reported. In all of them we exclude from the analysis an initial interval of time from laser-pulse application up to the moment t_0 when carrier concentration is roughly 10^{16} cm^{-3}, so that the system is on the metallic side of the Mott transition, and can be treated as an internally thermalized two-component (electron-hole) Fermi liquid.

(a) For the case of Ref. 22 we introduce a rectangular profile laser pulse of 1-ps duration and intensity of 1.0×10^{15} photons per cm^2 and photon energy $\hbar\omega_L$ of 4 eV. Lattice temperature is 300 K and excess energy per pair is 2.6 eV. Taken the initial time at 0.1 ps (zero time at the beginning of the pulse), estimating a production of 20 LO phonons per pair up to t_0 and using energy conservation in the form $3k_B[T_{excess} - T(t_0)] = 20\hbar\omega_0$, we find $T(t_0) = 7130$ K. $T_{LO}(t_0)$ is practically unaltered compared with the equilibrium value, since the number of phonons produced in excess of equilibrium is much smaller than $N_{eq} \sim 2 \times 10^{21}$ cm^{-3}. For the LO-phonon energy relaxation time, due to anharmonic processes, we take $\tau = 30$ ps; this value allows for a good fitting of experimental data at long delay times. All other parameters are given in Table I. The thermodynamic evolution of the semiconductor plasma is described by Figs. 1 and 2. The
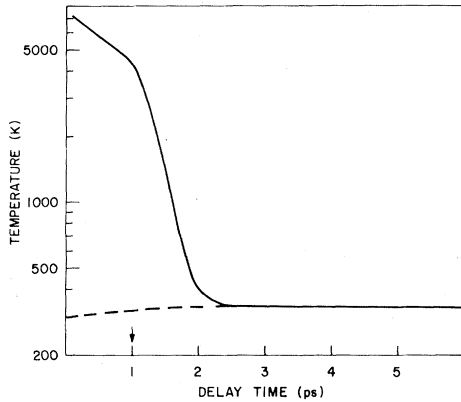
FIG. 1. Evolution of carrier (solid line) and LO-phonon (dashed line) effective temperatures calculated in the conditions given in Sec. IV, case (a).
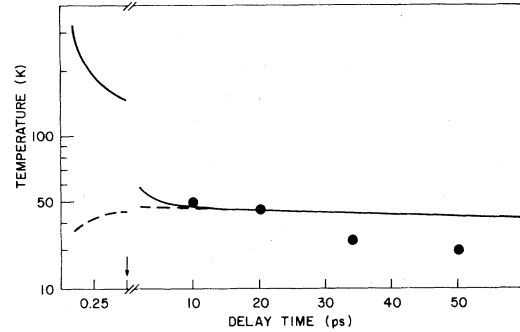

FIG. 3. Evolution of carrier (solid line) and LO-phonon effective temperatures calculated in the conditions given in Sec. IV, case (b). Closed circles are experimental points.

first shows the time dependence of carriers and LO-phonon quasitemperatures, and the second that of the quasichemical potentials.

(b) For the case of Ref. 23, $t_p = 0.5$ ps, laser intensity is 3.8×10^{13} photons per cm^2, $\hbar\omega_L = 1.64$ eV, excess energy per pair is 120 meV, and $T_0 = 10$ K. Using energy conservation and estimating a production of 1 LO phonon per pair up to $t_0 = 0.1$, when $n(t_0) = 4.2 \times 10^{16}$ cm^3, we find $T(t_0) = 322$ K and $T_{LO}(t_0) = 36$ K. We take $\tau = 60$ ps. Figures 3 and 4 describe the thermodynamic evolution of this system.

(c) For the case of Ref. 24 $t_p = 25$ ps, laser intensity is $\simeq 5 \times 10^{16}$ photons per cm^2, $2\hbar\omega_L = 2.33$ eV

(two-photon absorption processes), excess energy per pair is 0.811 eV, and $T_0 = 7.2$ K. Estimating a production of 6 LO phonons per pair up to $T_0 = 1$ ps, when $n(t_0) = 8 \times 10^{15}$ cm^{-3}, we find $T(t_0) = 2283$ K and $T_{LO}(t_0) = 37$ K. Relaxation time τ, same as in (b). Figures 5 and 6 show the results for this system.

Figures 7–12 describe the evolution of the rate of energy transfer through the different relaxation channels. Based on these results we proceed in the next section to draw several conclusions on the behavior of ultrafast transient relaxation phenomena in polar semiconductors.

V. DISCUSSION AND CONCLUSIONS

The numerical results presented in Figs. 1–12, however, specifically referred to GaAs, can be ex-
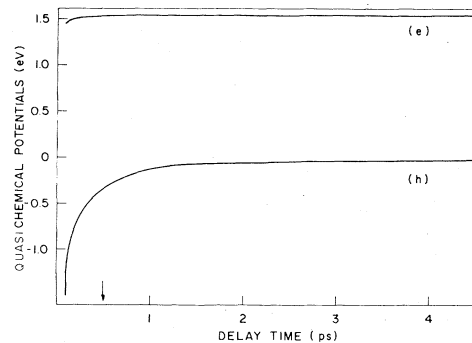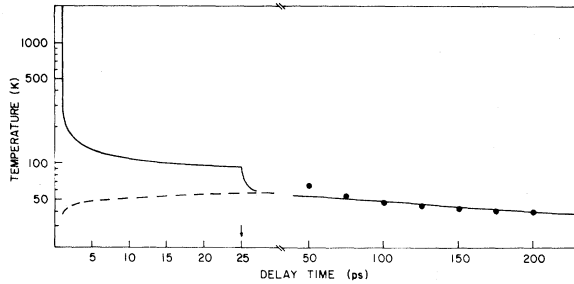

FIG. 2. Evolution of electron (e) and hole (h) quasichemical potentials calculated in the conditions given in Sec. IV, case (a). Zero of energy at top of the valence band.

FIG. 4. Evolution of electrons (e) and hole (h) quasichemical potentials calculated in the conditions given in Sec. IV, case (b). Zero of energy at top of valence band.

FIG. 5. Evolution of carrier (solid line) and LO-phonon (dashed line) effective temperatures calculated in the conditions given in Sec. IV, case (c). Closed circles are experimental points.

pected to be quite similar in scope for most intermediate to strong polar semiconductors, e.g., CdS and CdSe which have also been the object of experimental studies with ultrafast laser spectroscopy. A quite general characteristic appears to be the very rapid relaxation of the carriers' excess energy towards the LO-phonon system via Fröhlich interaction; the typical relaxation time is of the order of a picosecond. The overall picture of ultrafast transient behavior in photoexcited polar semiconductors depends upon experimental conditions:

(i) When an experiment is performed at room temperature, the concentration of phonons in equilibrium is of the order of 10^{21} cm^{-3}. For not-too-long laser pulses, producing pair concentrations up to 10^{19} per cm^3, the number of LO phonons created in excess of equilibrium is small. Then carrier quasitemperature rapidly decreases, and in a few picoseconds becomes equal to the LO-phonon quasi-
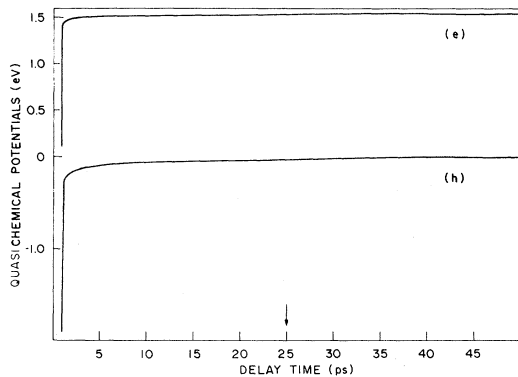

FIG. 6. Evolution of electron (e) and hole (h) quasi-chemical potentials calculated in the conditions given in Sec. IV, case (c). Zero of energy at top of valence band.
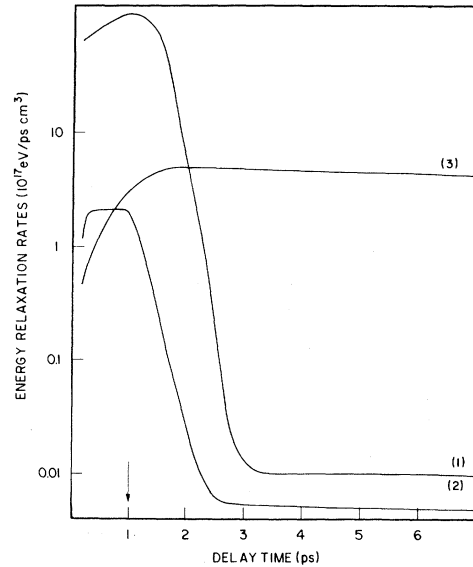

FIG. 7. Rate of energy relaxation of carriers to LO-phonon (1) and A-phonon (2) fields and of LO-phonon energy due to anharmonic processes (3) in case (a).

temperature, at a value slightly above T_0. From then on both systems, mutually thermalized, relax to final equilibrium with the lattice. This is the case of the experiment of Ref. 22, and Fig. 1 shows the evolution of quasitemperatures. The kinetics of relaxa-
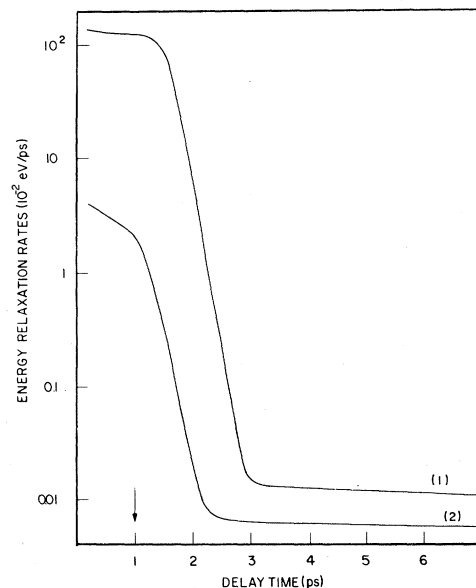

FIG. 8. Rates of energy relaxation per electron-hole pair of carriers to LO-phonon (1) and A-phonon (2) fields in case (a).
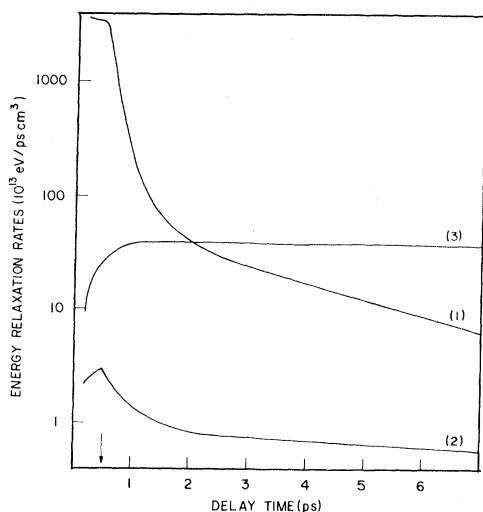
FIG. 9. Rate of energy relaxation of carriers to LO-phonon (1) and A-phonon (2) systems, and of LO-phonon energy due to anharmonic processes (3) in case (b).

FIG. 11. Rate of energy relaxation of carriers to LO-phonon (1) and A-phonon (2) fields, and of LO-phonon energy due to anharmonic processes (3) in case (c).

tion is described by Figs. 7 and 8. It can be noted that the rate of energy relaxation of carriers due to interaction with the LO phonon is a factor of 100 larger than that due to interaction with A phonons during and immediately after the laser pulse, but both become comparable a couple of picoseconds after pulse completion. The rate of LO-phonon excess energy relaxation via anharmonic interaction in-
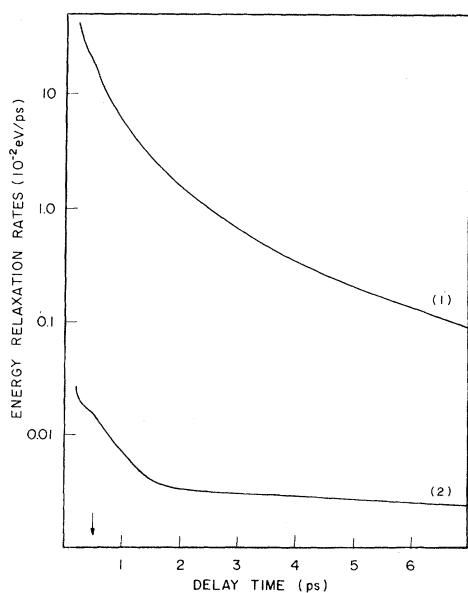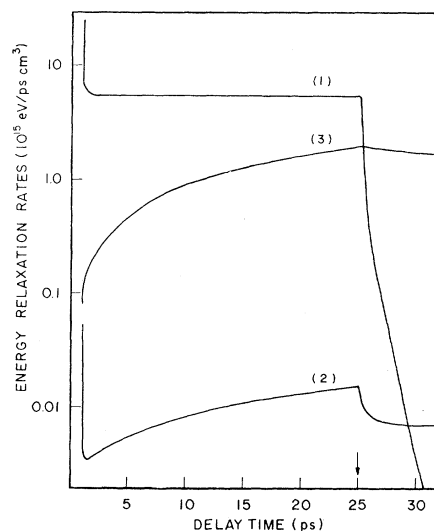
creases while the number of LO phonons increases up to the point of thermalization with carriers, to slowly decrease next following the decreasing value of T_{LO}. Quasichemical potentials (Fig. 2) also show a rapid variation during and roughly a picosecond

FIG. 10. Rate of energy relaxation per electron-hole pair of carriers to LO-phonon (1) and A-phonon (2) fields in case (b).
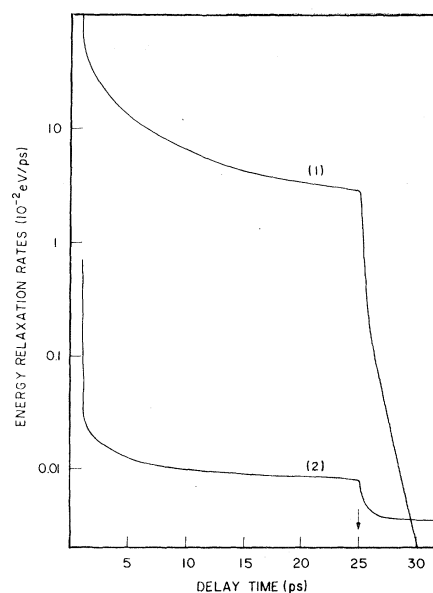
FIG. 12. Rate of energy relaxation per electron-hole pair of carriers to LO-phonon (1) and A-phonon (2) fields in case (c).

after laser pulse due to the rapid variation of carrier quasitemperature in this interval; the electron-hole gas changes from an initially classical to a final degenerate quantum gas. These results quite agree with those derived through the study of time-resolved reflectivity measurements.[22]

(ii) When reservoir temperature T_0 is low, under high levels of excitation the number of LO phonons in excess of equilibrium, produced by carriers cascading down the band energies, is usually larger than the equilibrium number. $T_{LO}(t_0)$ is then larger than T_0, and is increasing while carrier temperature decreases during application of the laser pulse, and both become equalized soon after pulse. From then on the common quasitemperature decreases towards the total equilibrium value T_0 at a very slow pace. This explains the long near plateau in the curve of T vs t noted in several experiments.[23-25] Figures 3 and 5 show the evolution of quasitemperatures in the conditions of the experiments of Refs. 23 and 24; closed circles are experimental values obtained through fitting of transmission[23] and absorbence[24] spectra. Figures 4 and 6 show the quasichemical potentials as a function of time; the initial rapid variation accompanies that of $T(t)$, and it can be observed that in both cases the electron-hole gas is always a degenerate quantum gas. It has been argued[23] that at high densities ($> 10^{18}$ cm^{-3}) the carriers can no longer be described by a thermal distribution, that seemed to be indicated by anomalies of behavior in the high-energy side of the transmission spectra. There is no reason to expect a deviation of carriers from a thermalized distribution in energy space; the reported anomaly seems to be an apparent one due to LO-phonon assisted processes. This type of effect has already been noted in other experiments.[26]

Figures 9-12 describe the kinetic of relaxation in both cases. The dependence on time of the rates of energy loss via the different relaxation channels follow a general pattern similar to that of (i) (Figs. 10 and 11). Agreement with experimental data is good in the case of Fig. 5 but less satisfactory in Fig. 3.

(iii) Relaxation of carriers to final equilibrium occurs mainly through the indirect channel of carriers—LO phonons—acoustic phonons. The relaxation of LO phonons to the lattice is mediated by anharmonic interaction, which plays here an important role because of the departure of the LO-phonon field amplitude of the equilibrium value. Relaxation of carriers through a direct channel mediated by deformation potential interaction is much slower, beginning to be relevant only after mutual thermalization of carriers and LO phonons. In the absence of anharmonic effects there results a strong bottleneck of the carrier relaxation due to the high excitation of

optical phonons. The more effective this channel, i.e., shorter values of τ, the more rapid the relaxation of the HEPS system towards final equilibrium.

We recall the shortcomings of the calculation: (a) use of a rectangular pulse profile; a more realistic one should smooth out the curves for the different quantities during and after pulse (end of pulse indicated by an arrow in all figures), (b) uncertainty concerning the initial values of the nonequilibrium thermodynamic parameters, and (c) use of a common temperature for all LO-phonon modes at the very early stages of relaxation processes. Further, it must be borne in mind that at not too short delay times, typically when approaching the nanosecond scale, other contributions, neglected in the present calculation, need to be incorporated in the scattering operators, e.g., self-absorption and induced recombination become relevant when n approaches the equilibrium value at temperature T_0. The hypothesis used in the calculation—the A phonons remain constantly in equilibrium at reservoir temperature T_0—also deserves a comment. A phonons are warmed up as a result of energy transfer from, mainly, the relaxation channel governed by anharmonic interactions with LO phonons. For GaAs samples with an active volume with average linear dimensions of a few micrometers, and using typical values for thermal conductivity and specific heat, we find that cooling by heat diffusion occurs in the (10—100)-nsec scale for lattice temperatures ranging from 10 to 300 K. Hence, in principle, A-phonon heating needs to be considered. However, if $T_A(t)$ is the instantaneous A-phonon effective temperature, and C_A and C_{LO} are the contributions to the instantaneous specific heat from A and LO phonons, respectively, then

$$\left| \frac{dT_A}{dT_{LO}} \right| = \left| \frac{\dot{T}_A}{\dot{T}_{LO}} \right| = \frac{C_{LO}}{C_A} \left| \frac{-J_{1A}-J_{4AN}}{-J_{1LO}+J_{4AN}} \right| ,$$

and since the absolute value of the ratio of collision operators is less, or at most of the order of 1, and considering that C_{LO}/C_A is much smaller than 1 at low temperatures, or near 1 at room temperature, two situations can be distinguished. At low temperatures and not too long delay times, T_A should increase less than T_{LO}, while at intermediate to room temperature both effective temperature increase in a similar way, but only slightly above reservoir temperature, for the reasons already discussed in the main text. Consequently, the approximation used, $T_A = T_0$, does not significantly alter the relaxation pattern described here.

In conclusion we may say that techniques of ultrafast laser light spectroscopy in conjunction with nonequilibrium statistical mechanics methods, yielding nonlinear transport equations for the description

of kinetic and relaxation processes, provide a very powerful tool for the study of picosecond responses of semiconductor systems. Besides the interest in the comprehension of the basic physical problems involved, there exists a parallel technological interest since performance of semiconductors electronic devices is ultimately determined by how fast they operate. Development of this high-speed technology requires one to explore semiconductor behavior on picosecond and subpicosecond time scales.

[1]K. Hess and N. Holonyak, Physics Today 33, 40 (1980); C. V. Shank and D. H. Auston, Science 215, 797 (1982).

[2]See, for example, references quoted in R. Luzzi and L. M. C. Miranda, Phys. Lett. C 43, 423 (1979); M. Voos, R. Leheny, and J. Shah, Handbook on Semiconductors, edited by T. S. Moss (North-Holland, Amsterdam, 1980); C. Klingshirn and H. Haug, Phys. Lett. C 70, 315 (1981).

[3]E. M. Conwell, in Solid State Physics, Suppl. 9, edited by H. Ehrenreich, F. Seitz, and D. Turnbull (Academic, New York, 1967), Vol. 20, p. 1.

[4]E. T. Jaynes, Statistical Physics, edited by K. W. Ford (Benjamin, New York, 1963); Phys. Rev. 106, 620 (1957); 108, 171 (1957).

[5]B. Robertson, Phys. Rev. 144, 151 (1966); 160, 175 (1968); in The Maximum Entropy Formalism, edited by M. Tribus and D. Levine (MIT Press, Cambridge, 1978).

[6]D. N. Zubarev, Fortschr. Phys. 18, 125 (1970); Neravnovesnaia Staticheskaia Termodinamika (Nauka, Moscow, 1971) [English translation: Nonequilibrium Statistical Thermodynamics, Studies in Soviet Science Series, edited by P. Gray and P. J. Shephard (Consultants Bureau, New York, 1974)].

[7]R. Luzzi and A. R. Vasconcellos, J. Stat. Phys. 23, 539 (1980).

[8]N. N. Bogoliubov, in Studies in Statistical Mechanics, edited by I. de Boer and G. E. Uhlenbeck (North-Holland, Amsterdam, 1962), Vol. I; see also G. E. Uhlenbeck, in Lectures in Statistical Mechanics, edited by M. Kac (American Mathematical Society, Providence, 1963).

[9]S. V. Peletminskii and A. A. Yatsenko, Zh. Eksp. Teor. Fiz. 53, 1327 (1967) [Sov. Phys.—JETP 26, 773 (1968)].

[10]V. P. Kalashnikov, Teor. Mat. Fiz. 35, 127 (1978) [Theor. Math. Phys. (USSR) 35, 362 (1978)].

[11]P. Glansdorff and I. Prigogine, Thermodynamics of Structure, Stability and Fluctuation (Interscience, New York, 1971).

[12]This is a form to introduce the dynamic condition for dissipativity, I. Prigogine, Nature (London) 246, 67 (1973).

[13]N. N. Bogoliubov, Lectures on Quantum Statistics (Gordon and Breach, New York, 1970), Vol. II.

[14]R. Luzzi and A. R. Vasconcellos, in Semiconductor Processes Probed by Ultrafast Laser Spectroscopy, edited by R. R. Alfano (Academic, New York, in press).

[15]R. Luzzi and A. R. Vasconcellos, J. Raman Spectrosc. 10, 28 (1981).

[16]A. R. Vasconcellos and R. Luzzi, Phys. Rev. 22, 6355 (1980).

[17]D. von der Linde, J. Kuhl, and J. Klingenberg, Phys. Rev. Lett. 44, 1505 (1980).

[18]For a more detailed discussion of application of the method to open systems see J. Seke, Phys. Rev. A 21, 2156 (1980).

[19]A. C. Algarte, A. R. Vasconcellos, and R. Luzzi (unpublished).

[20]In Ref. 6, see Chap. IV, Sec. 25.

[21]R. S. Turtelli, R. B. de Castro, and R. C. C. Leite, Solid State Commun. 16, 169 (1975).

[22]C. V. Shank, D. H. Auston, E. P. Ippen, and O. Teschke, Solid State Commun. 26, 567 (1978).

[23]R. F. Leheny, J. Shah, R. L. Fork, C. V. Shank, and A. Migus, Solid State Commun. 31, 809 (1979).

[24]D. von der Linde and R. Lambrich, Phys. Rev. Lett. 42, 1090 (1979).

[25]H. Yoshida, H. Saito, and S. Shionoya, Phys. Status Solidi B 104, 331 (1981); M. Pugnet, A. Cornet, J. Collet, M. Brousseau, B. S. Razkirin, and G. M. Michailov, Solid State Commun. 36, 85 (1980).

[26]J. G. Ramos and R. Luzzi, Solid State Commun. 14, 1275 (1974).